A New Approach to SINR-based Reliability Analysis of IEEE 802.11 Broadcast Ad Hoc Networks

Xiaomin Ma, Jing Zhao, Yanbin Wang, Tingyu Zhang, and Zhijuan Li

***Abstract*—This letter proposes a new approach to the reliability analysis of IEEE 802.11 one-dimensional (1-D) broadcast mobile ad hoc networks. The approach finds a simple and effective way to derive the distribution of signal-to-interference-to-noise ratio (SINR) on each receiver, which is required for evaluation of the reliability metrics and the channel capacity. Having observed that the effective interference area depends on a given SINR threshold, the SINR distribution derivation is converted to estimating the SINR threshold related interference areas that are dynamically changed in a communication channel. The analysis is applied to two network configurations for example, and it is cross validated by the extensive simulations. Compared with the previous models, the new approach is more general, more precise, and faster.**

***Index Terms*—Broadcast, Ad hoc networks, Interference, SINR, Quality of Service**

I. INTRODUCTION

IEEE 802.11 based broadcast ad hoc networks have been studied for many mission-critical applications such as vehicular safety messaging, military and crisis emergency management, and medical monitoring, etc. These applications require high quality of service (QoS) regarding how reliable the surrounding nodes are able to receive broadcast messages from a tagged node within the message lifetime. It is important to investigate the QoS of such systems analytically in the process of the design and the system upgrading (e.g., from 802.11p to 802.11bd [5]). On the other hand, many intelligent model-based systems call for accurate and fast analytical models for real-time optimization of the network parameters [4] [7]. Recently, a few signal-to-interference-to-noise ratio (SINR) based models have been proposed for the analysis of IEEE 802.11 vehicular ad hoc network (VANET) for safety message broadcast [1–3]. The models approached the QoS analysis of the VANET safety message broadcast under the fading channels through the derivation of the SINR distribution. However, due to the features of carrier sensing mechanism in the 802.11 channel access, there is no effective SINR-based model to quantify the QoS of such networks up to the date. The models in [1–2] assumed a fixed interference range of hidden terminals, which brings remarkable errors to the QoS evaluation, as shown in Section V. The stochastic geometry models [3] [8] approximated the behavior of the carrier sensing in 802.11 using ALOHA and Matern type II process. The accuracy of the models is sensitive to node density. Also, the models only apply to uniform Poisson networks under *Rayleigh* fading channel [3]. Furthermore, the models in [1–3] took many complex iterations and high-order integrations to derive the needed QoS results, which are very time consuming. Besides, all the current SINR-based models assume that communication systems adopt a hard-limiter SINR threshold for making decision on message receptions. However, many practical communication channels are often characterized by packet loss rate (PLR) in terms of the measured immediate SINR values, which is referred to as PLR(SINR) curve [7].

In this letter, a new effective SINR-based analytic approach is proposed to analyze the reliability and the capacity of IEEE 802.11 broadcast ad hoc networks. In the new approach, the SINR distribution derivation is divided into the evaluation of signal-to-interference ratio (SIR) distribution and the evaluation of signal-to-noise ratio (SNR) distribution in the *Nakagami* channel. Under a few reasonable assumptions, the SINR distribution analysis can be converted to evaluating the transmission probability of a node in an estimated interference area that is a dynamic function of communication distance and a specified SINR threshold. Then, the SINR distribution serves for the QoS analysis of the systems that adopt both the SINR threshold and the PLR(SINR) curves on the reception of transmitted messages. The new approach considers the impact of IEEE 802.11 MAC channel access, interferences from other nodes' transmissions, and noise.

II. PROBLEM FORMULATION AND ASSUMPTIONS

A. Problem Formulation

We consider a wireless broadcast ad hoc network where each node sends messages to its surrounding nodes in its transmission range regularly with a message generation rate (λ) and transmitting power (P_t). Each node also receives the broadcast messages from the surrounding nodes. All channel accesses and packet transmissions follow IEEE 802.11 carrier-sense multiple access (CSMA) protocol [9]. The QoS is degraded by message collisions and fading/shadowing in the communication channels. The collisions occur once other nodes transmit to a same receiver when a transmission is going on. Two types of the interference may cause the failure of message delivery in the networks: hidden terminal (HT) and concurrent transmission (CT) [7]. CT occurs when any of the nodes within a tagged node's carrier sensing range (r_E) starts to transmit at the same slot on which the tagged node starts its transmission. HT occurs when any of the nodes out of the tagged node's carrier sensing range sends a message to the same receiver at the same time while the tagged node is transmitting. Also, the QoS is degraded by the *Nakagami* fading/shadowing with path loss. It is important that the network is able to provide the safety services with the guaranteed reliability. In order to evaluate the reliability metrics such as packet delivery probability (*PRP*) and packet reception ratio (*PRR*) in this regard, the SINR distribution needs to be evaluated.

B. Assumptions

We assume that the IEEE 802.11 driven message broadcast networks work under the following scenarios.

This is the author's version of an article that has been published in this journal. Changes were made to this version by the publisher prior to publication.
The final version of record is available at http://dx.doi.org/10.1109/LCOMM.2020.3026300

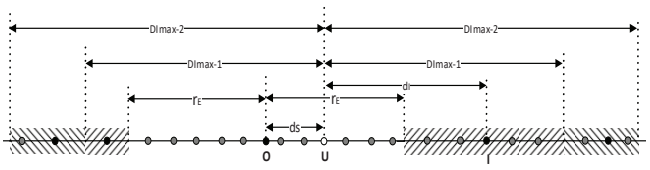

Fig. 1 General interfering scenario for MANET message broadcast

1) A 2-D strip-like area or a straight road is approximated by a one-dimensional (1-D) line, as shown in Fig. 1.
2) Two types of node distributions are assumed and considered for two potential traffic patterns: (i) Denote Y_M as the sum of M neighboring node inter-distance to the tagged node, probability density function (PDF) of Y_M follows the log-normal distribution (LND) with mean μ and variance σ [1–2]. This node distribution is a good approximation of nodes on urban roads. (ii) All mobile nodes are placed on 1-D line according to homogeneous Poisson process (HPP) with the density of vehicles β (in nodes per meter) [3] [8]. This node distribution is a good approximation of nodes on free roads.
3) All nodes are treated as homogeneous with identical body length L_V and transmission power P_t.
4) *Nakagami* fading model with exponential path-loss is assumed for the wireless communication channel.

Then, PDF of the power P_r received from a receiver with distance d away from a source node is rewritten as

$$f_{P_r|d}(x) = \frac{1}{\Gamma(m)}\left(\frac{m}{\overline{P}_r(d)}\right)^m x^{m-1}\exp\left(-\frac{mx}{\overline{P}_r(d)}\right), \quad (1)$$

where $\Gamma()$ is the Gamma function, and m is the fading parameter. $\overline{P}_r(d) = P_t\eta\left(\frac{d_0}{d}\right)^\alpha$ (d_0 is the reference distance for the far-zone field, α is the path-loss exponent, and η is a transceiver-determined constant) is the mean value determined by the path-loss.
5) A deterministic carrier sensing range (r_E) is assumed in the analysis, where $r_E = d_0\sqrt[\alpha]{P_t\eta/P_{th}}$ [1], and P_{th} is the clear channel assessment (CCA) sensitivity.
6) Collisions and fading are independent of each other, so that the derivation of collision probability and error rate due to fading can be separately carried out. This assumption is theoretically true as $m = 1$ in *Nakagami* fading channel [8], and is a reasonable approximation as m is not equal to 1, which can be verified by the numerical results later.
7) The interference ranges are open as opposed to the fixed interference range (r_E) in [1–2]. The distance between an interferer and the tagged transmitter is no longer than I_{max}.

III. ANALYSIS OF SINR DISTRIBUTION

To evaluate the reliability and other QoS metrics, the SINR distribution should be derived. Given a SINR threshold θ, the SINR distribution, cumulative density function (CDF), can be formulated as

$$F_{SINR}(\theta) = Pr(SINR < \theta) = Pr\left(\frac{P_r}{N + \sum_i I_i} < \theta\right),$$

where P_r is the power strength of signal from a sender on a receiver, I_i is the power strength of i's interference signal on the receiver, and N is the average power of noise.

We observe that the immediate SINR value depends on both the distance between a transmitting node and a receiving node and the distance between an interferer and the receiving node. Also, due to the carrier sensing mechanism in IEEE 802.11 driven networks, once an interfering node is transmitting, no other nodes within the transmitting node's carrier sensing range will be allowed to transmit. As shown in Fig. 1, given a transmitting (tagged) node O sending out messages (packets), U is one of the receivers with distance d_s to O, and I is an interfering node with distance d_I to the receiver. In *Nakagami* channel characterized by Eq. (1), the mean receiving power decays exponentially with distance between the transmitter and the receiver. Thus, the expected SINR expression in the IEEE 802.11 broadcast ad hoc network becomes

$$SINR = \frac{P_r(d_s)}{N + I(d_I)} = \frac{P_t\eta\left(\frac{d_0}{d_s}\right)^\alpha}{N + P_t\eta\left(\frac{d_0}{d_I}\right)^\alpha} < \theta$$

Keeping above inequality in our mind, given a tagged node O sending a packet to a receiver U, we observe and deduce that the effective range of the interference in which any node I's transmission causes the immediate SINR value measured on node U less than the specified SINR threshold θ is limited and dynamically changed with the distance d_s and the threshold θ. The smaller $d_s(\theta)$ is, the smaller the interference range is.

Next, we analyze the SINR distribution of a transmission in IEEE 802.11 broadcast networks with interference as well as noise in the *Nakagami* wireless channel. From assumption (6), the SINR analysis can be divided into the SIR analysis and the SNR analysis. The impact of the interference on SINR is studied through evaluating the transmission probabilities of nodes inside and outside of the tagged node's carrier sensing range, respectively.

A. SINR Distribution Accounting For Interference

Knowing that only one transmission from the interference area beyond the carrier sensing range (either one side of two shaded areas in Fig. 1) is allowed, define D_{Imax-1} as the maximum distance between an receiver and the farthest interferer whose transmission causes SIR less than the specified threshold, which can be decided by

$$SIR = \frac{P_t\eta\left(\frac{d_0}{d_s}\right)^\alpha}{P_t\eta\left(\frac{d_0}{D_{Imax-1}}\right)^\alpha} = \theta \quad (2)$$

$$D_{Imax-1} = (\theta)^{\frac{1}{\alpha}} d_s \quad (3)$$

There is other possibility that two nodes beyond the above shaded area transmit from two sides simultaneously to result in SIR less than θ. Define D_{Imax-2} to be the distance between the receiver and the farthest node in the new shaded areas, in which any two-node transmissions can cause the immediate SIR less than θ, which is approximately decided by

$$SIR = \frac{P_t\eta\left(\frac{d_0}{d_s}\right)^\alpha}{2P_t\eta\left(\frac{d_0}{D_{Imax-2}}\right)^\alpha} = \theta \quad (4)$$

$$D_{Imax-2} = (2\theta)^{\frac{1}{\alpha}} d_s \quad (5)$$

Therefore, the derivation of the SIR distribution can be converted to the evaluation of the probability that the interfering

This is the author's version of an article that has been published in this journal. Changes were made to this version by the publisher prior to publication.
The final version of record is available at http://dx.doi.org/10.1109/LCOMM.2020.3026300

nodes within the distance constraint (D_{Imax-1} or D_{Imax-2}) transmit when U is receiving a message from O. The interfering nodes in different areas will affect U's receiving message to different degree with different probabilities. In practical communication systems, interference from nodes beyond certain distance I_{max} may be too weak to be considered. So, $D_{Imax} = min\{D_{Imax-1}, I_{max}\}$; and $I_{max} \geq D_{Imax-2} > D_{I-max}$.

Here, we introduce two probabilities that facilitate the derivation of SINR distribution from the Semi-Markov analysis of IEEE 802.11 broadcast [6]. First, the probability π_0 that a node starts to transmit in the beginning of a time slot immediately after the backoff process, which is expressed as

$$\pi_0 = \frac{2\sigma[\rho + q_b(1-\rho)]}{[\rho + q_b(1-\rho)][(t_s + p_b T)W_0 + (\sigma - p_b T)] + 2T + 2(1-\rho)(\frac{1}{\lambda} + AIFS)}$$

where T is the time duration for one packet transmission, t_s is slot duration, ρ is the probability that there are packets in the queue of the tagged node, p_b is the probability that the channel is detected busy in one time slot by the tagged node, q_b is the probability that the channel is detected busy in AIFS time by the tagged node, and AIFS is a time period of arbitration inter-frame space of IEEE 802.11p MAC. Second, considering node O and node I are out of mutual carrier sensing range, I's transmission could occur at any time of O's transmission. According to [6], the probability that a node I in the shaded area transmits during the vulnerable period of the transmission from the tagged node O is evaluated as

$$p_t = \pi_{XMT} \frac{2(T - AIFS)}{T}, \tag{6}$$

where π_{XMT} is the steady-state probability that a node is in transmission state, which is derived in [6].

$$\pi_{XMT} = \frac{T}{\sigma[\rho + q_b(1-\rho)]}\pi_0.$$

Next, we consider how the interfering nodes outside of O's carrier sensing range degrade O's transmissions to U from the perspective of SIR, as shown in Fig. 1. Given a transmission distance d_s, the probability that SIR on U is less than the specified threshold θ is equal to the probability that at least one of nodes in the symbol "/" marked shaded HT areas [r_E, $D_{Imax} - r_E + d_s$] or [$-D_{Imax} + d_s$, $-r_E$] transmits. So, the probability that at least one transmission from either side of the hidden interference areas for two types of node distributions can be described as

$$P_{sh}(d_s) = Pr\{SIR < \theta | d_s\} = \begin{cases} 1 - (1-p_t)^{N_{ht}}, if\ LND \\ 1 - e^{-\beta p_t D_{ht}}, if\ HPP \end{cases}. \tag{7}$$

Considering the possibility that D_{Imax} could be smaller than the sensing range r_E for some situations, the total hidden terminal area D_{ht} from both sides for HPP node distribution can be expressed as

$$D_{ht}^1 = max(D_{Imax} - r_E + d_s, 0),$$
$$D_{ht}^2 = max(D_{Imax} - r_E - d_s, 0),$$
$$N_{ht} = D_{ht}^1 + D_{ht}^2.$$

According to [1], the average number of hidden terminals N_{ht} for LND node distribution can be estimated as

$$N_{ht}^1 = \sum_{n=1}^{N_v^1} n \cdot Pr\{Y_n \leq r_E\} Pr\{Y_n + D_{n+1} > r_E | Y_n \leq r_E\}$$

$$N_{ht}^2 = \sum_{n=1}^{N_v^2} n \cdot Pr\{Y_n \leq r_E\} Pr\{Y_n + D_{n+1} > r_E | Y_n \leq r_E\}$$
$$N_{ht} = N_{ht}^1 + N_{ht}^2,$$

where $N_v^1 = \lfloor D_{ht}^1 / L_V \rfloor$, and $N_v^2 = \lfloor D_{ht}^2 / L_V \rfloor$. D_{n+1} is the distance between nth node and $n+1$th node.

On the other hand, there is the possibility that at least two of nodes from two sides of the symbol "\" marked shaded HT areas [$-D_{Imax-2}+d_s$,$-D_{Imax}+d_s$] and [$D_{Imax}+d_s$,$D_{Imax-2}+d_s$] transmit simultaneously, which also could cause the SNR value less than the threshold θ.

$$P_{hc}(d_s) = \begin{cases} (1-(1-p_t)^{N_{ht}^{21}})(1-(1-p_t)^{N_{ht}^{22}}), if\ LND \\ (1-e^{-\beta p_t D_{ht}^{21}})(1-e^{-\beta p_t D_{ht}^{22}}), if\ HPP \end{cases} \tag{8}$$

where

$$D_{ht}^{21} = [max(D_{Imax-2} - max(D_{Imax}, r_E + d_s), 0)],$$
$$D_{ht}^{22} = [max(D_{Imax-2} - max(D_{Imax}, r_E - d_s), 0)].$$

From the log-normal distribution described in [1], we have

$$N_{ht}^{21} = \sum_{n=1}^{N_v^{21}} n \cdot Pr\{Y_n \leq r_E\} Pr\{Y_n + D_{n+1} > r_E | Y_n \leq r_E\}$$

$$N_{ht}^{22} = \sum_{n=1}^{N_v^{22}} n \cdot Pr\{Y_n \leq r_E\} Pr\{Y_n + D_{n+1} > r_E | Y_n \leq r_E\}$$

where $N_v^{21} = \lfloor D_{ht}^{21} / L_V \rfloor$, and $N_v^{22} = \lfloor D_{ht}^{22} / L_V \rfloor$.
In addition, the concurrent transmission takes place when any of the nodes within r_E range of the tagged node starts its transmission. Then, considering the possibility that D_{Imax} could be smaller than the sensing range r_E for some transmission situations, the probability that at least one concurrent collision occurs can be evaluated as

$$P_{cc}(d_s) = \begin{cases} 1 - (1-\pi_0)^{N_{cc}}, if\ LND \\ 1 - e^{-\beta D_{cc} \pi_0}, if\ HPP \end{cases} \tag{9}$$

$$D_{cc}^1 = min(D_{Imax}, r_E - d_s)$$
$$D_{cc}^2 = min(D_{Imax}, r_E + d_s)$$
$$D_{cc} = D_{cc}^1 + D_{cc}^2$$

$$N_{cc}^1 = \sum_{n=1}^{N_v^{c1}} n \cdot Pr\{Y_n \leq r_E\} Pr\{Y_n + D_{n+1} > r_E | Y_n \leq r_E\}$$

$$N_{cc}^2 = \sum_{n=1}^{N_v^{c2}} n \cdot Pr\{Y_n \leq r_E\} Pr\{Y_n + D_{n+1} > r_E | Y_n \leq r_E\}$$
$$N_{cc} = N_{cc}^1 + N_{cc}^2$$

where $N_v^{c1} = \lfloor D_{cc}^1 / L_V \rfloor$, and $N_v^{c2} = \lfloor D_{cc}^2 / L_V \rfloor$.

B. SINR Distribution Accounting For Noise

Without taking interferences into account, SINR drops to SNR:

$$SINR = \frac{P_r}{N}, \tag{10}$$

where P_r is the receiving power strength, N is the average power strength of noise. Correlate the above SNR equation into Eq. (1) (PDF of *Nakagami* fading), we have

$$\begin{aligned} P(Y \leq \theta | d_s) &= F_{SNR|d_s}(\theta, \omega, m) \\ &= \frac{(Nm)^m}{\Gamma(m)\omega^m} \int_0^{\theta} z^{(m-1)} e^{-N(\frac{m}{\omega})z} dz \\ &= \frac{(Nm)^m}{\Gamma(m)} \int_0^{\frac{\theta}{\omega}} z^{(m-1)} e^{-Nmz} dz \end{aligned} \tag{11}$$

On the average, θ is equal to the SNR value when it is measured at the communication distance R_c. In addition, the carrier sensing threshold P_{th} is measured at a node with the

carrier sensing range r_E. According to the path loss law, we have

$$\frac{\theta N}{P_{th}} = \left(\frac{r_E}{R_c}\right)^{\alpha}. \tag{12}$$

Then,

$$\frac{\theta}{\omega(d_s)} = \frac{1}{N}\left(\frac{d_s}{R_c}\right)^{\alpha} = \frac{\theta}{P_{th}}\left(\frac{d_s}{r_E}\right)^{\alpha} \tag{13}$$

Thus, CDF of SNR is expressed as

$$\begin{aligned} P(Y \le \theta | d_s) &= F_{SNR|d}(\theta, \omega, m) \\ &= \frac{(Nm)^m}{\Gamma(m)} \int_0^{\frac{\theta}{P_{th}}\left(\frac{d_s}{r_E}\right)^{\alpha}} z^{(m-1)} e^{-Nmz} dz \end{aligned} \tag{14}$$

Assuming independence of the above three factors affecting the message delivery from O to U, the CDF of SINR given a distance d_s can be summarized as

$$\begin{aligned} &F_{SINR|d_s}(\theta) = \Pr(SINR < \theta | d_s) \\ &= 1-(1-P_{sh}(d_s))(1-P_{hc}(d_s))(1-P_{cc}(d_s))(1-P(Y \le \theta | d_s)) \end{aligned} \tag{15}$$

Then, the PDF of SINR given the distance d_s is evaluated as

$$f_{SINR|d_s}(s) = \frac{dF_{SINR|d_s}(s)}{ds} \tag{16}$$

IV. RELIABILITY DERIVATION

Having derived the SINR distribution, the following reliability metrics are defined and evaluated.

1) Packet delivery probability (*PRP*), defined as the probability that a receiver successfully decodes a packet from a source node with distance d_s to the receiver, is evaluated as the probability that the conditional SINR measured at the receiver is higher than the given threshold and the received signal is stronger than the reception threshold R_{th}, which is expressed as

$$PRP(d_s, \theta) = \Pr\{SINR \ge \theta | d_s, P_r \ge R_{th} | d_s\}$$

So, we have

$$\begin{aligned} PRP(d_s, \theta) &= \Pr\{SINR \ge \theta | P_r \ge R_{th}, d_s\} \Pr\{P_r \ge R_{th} | d_s\} \\ &= (1 - F_{SINR|d_s}(\theta))(1 - \int_0^{R_{th}} f_{P_r|d_s}(x)dx). \end{aligned} \tag{17}$$

In the real wireless communication systems, the observation that the measured SINR is greater than the given threshold does not lead necessarily to a successful delivery of the messages. In many practical cases, the wireless channels under various modulation and coding schemes (MCSs) are characterized by packet loss rate (PLR) as a function of the immediate SINR value [7]. Therefore, another way to receiving a message is implemented according to an experimentally derived PLR(SINR) curves instead of a fixed SINR threshold. The *PRP* evaluation based on the given PLR(SINR) curves can also be derived through the above SINR distribution:

$$PRP(d_s) = (1 - \int_0^{\infty} PLR(s) f_{SINR|d_s}(s) ds)(1 - \int_0^{R_{th}} f_{P_r|d_s}(x)dx) \tag{18}$$

where $PLR(s)$ reflects a PLR function given a SINR value s.

2) Packet reception ratio (*PRR*), defined as the percentage of receivers in a range that are free from the transmission errors once a broadcast message is sent out, can be evaluated as the percentage of the receivers within d_s that are free from transmission errors.

$$PRR(d_s, \theta) = \frac{1}{d_s} \int_0^{d_s} PRP(x)dx \tag{19}$$

3) Link capacity. The distribution and expectation of the link capacity is defined and expressed by Eq. (12) and Eq. (13) in [1].

V. NUMERICAL RESULTS AND DISCUSSIONS

To validate the new proposed analysis, Python is deployed for the theoretical computations and NS2 is deployed for the network simulations. In NS2 simulations, the communication nodes are distributed over the areas with length of 8500m. The maximum interference range is set as I_{max}=5000m, which is long enough to cover most potential interferers. The time resolution of the simulation is 1μs. The computer used for running the simulations and the analytic model is Dell Optiplex with CPU main frequency 2.4GHz,RAM size 16 GB.

A. Model Validation and Comparison with Previous Model: Hard-limiter SINR Threshold based Receiver

First, we consider an IEEE 802.11 driven VANET where nodes are distributed on a 2-D strip-like area according to the log-normal distribution. For the purpose of comparison, we reproduce the numerical results in [2], and adopt the same communication network parameters in [2] to test the new model.

Fig. 2 shows the *PRPs* and *PRRs* at the receivers in the same network. It is shown that the results (line) from the new model reasonably agree with the simulation results (symbols) with 95% confidence intervals (CIs). The average relative errors between the theoretical results from the new model and the corresponding simulation results are 7.7% (*PRP*), and 2.9% (*PRR*), respectively. The errors between the simulation results and the proposed analytic counterparts can be due to the assumptions in the analytic model on the node distribution and on the independence of the collision impact and the noise impact. In contrast, the average relative errors between the theoretical results in [2] (Fig. 3 in [2]) and the corresponding simulation results are 19.3% (*PRP*), and 8.9% (*PRR*), respectively. The simulation with the fixed interference range (by adjusting "PowerMonitorThresh_" in NS2) is also conducted. The simulation results (black symbols) agree with the theoretical *PRP* and *PRR* counterparts (blue line) derived in [2], which reveals the factor in the model [2] that causes the bigger errors: underestimation of the interference impact by confining the HT areas within r_E in the analytic model.

Fig. 3 depicts PDF of the link capacity derived from both the simulations and the new analytic model, and compared with that in [2] (Fig. 4 in [2]). From Fig. 3, we can see the remarkable difference between the PDF derived from new model and that derived from the model in [2]. Due to the underestimation of the interference impact with fixed HT area in [2], the link capacity in [2] is overestimated (the expected link capacity $E(C)_{new\ model}$=78Mbps, $E(C)_{old\ model}$=101Mbps).

Through the exhaustive tests, we observe that the new proposed model can derive one cycle of the reliability results within 0.5 seconds due to its lower computation complexity comparing to more than 1.3 hours for which the analytic models in [1–2] took to derive the same results.

B. Model Validation and Application Example: PLR(SINR) Curve based Receiver

Second, we consider the other broadcast ad hoc networks where each node is exponentially distributed with density β=0.1 nodes/m on a 1-D line and is equipped with wireless capability adopting the updated PHY layer parameters for

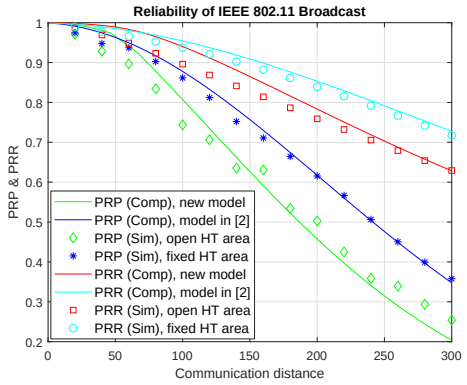

Fig. 2 Reliability (*PRP* and *PRR*) vs. distances (μ=2.548, σ=0.76, θ = 30)

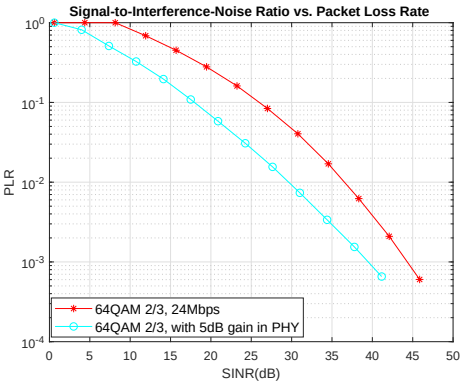

Fig. 4: PLR(SINR) curves in PHY layer

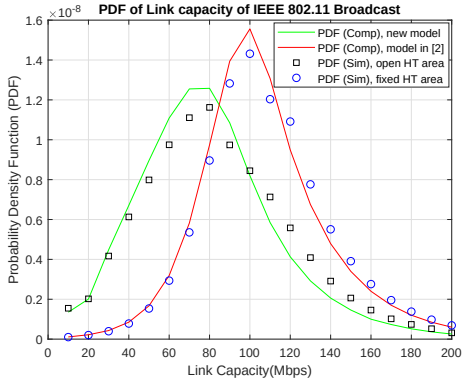

Fig. 3: Link capacity distribution (PDF) of IEEE 802.11 channel

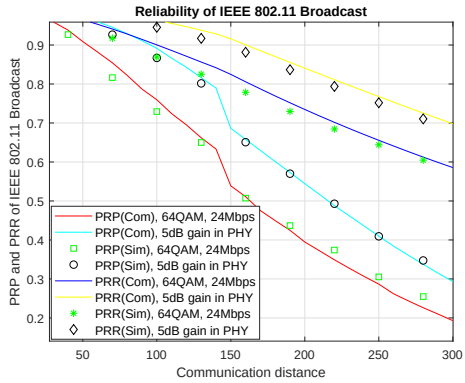

Fig. 5: PLR(SINR) curve based analysis of MAC reliability

OFDM based IEEE 802.11 [9]. Slot time t_s=13μs, AIFS=58μs, PHY preamble T_{H1}=32μs, PHY header T_{H2}= 8μs, symbol duration T_s=6.4μs, channel bandwidth B=10MHz, and backoff window size W=15. The communication network parameters are set as follows: transmission power of each node P_t=0.28183815 Watts, carrier sensing power strength P_{th}=R_{th}=5.127 15 $\times 10^{-11}$ Watts (clear channel assessment sensitivity for range 300m), N (noise_floor)=1.2589 $\times 10^{-13}$ Watts, the reference distance for the far-zone d_0=100 meters, loss-path constant η=1.637 26 $\times 10^{-9}$, *Nakagami* parameter m = 3 for d_s<50m, $m = 1.5$ for $50m \le d_s < 150m$, and $m = 1$ for $d_s \ge 150m$. As an example, the channel decoding error rates for 64QAM 2/3 24Mbps given packet length 200 bytes are characterized by a PLR(SINR) curve [7] as shown in Fig. 4 (red line). Assume that a certain performance gain (say 5dB) is introduced to the 64QAM channel in physical layer due to some new technologies such as low-density parity-check (LDPC) channel coding, or dual sub-carrier modulation (DCM) mode, etc. The channel with the gain can be characterized by the other curve in Fig. 4 (cyan line). From Fig. 4 we can see that the PLRs depend on the immediate measured SINR without a specific threshold. With the SINR distribution obtained by Eq. (15) and Eq. (16) and the two PLR(SINR) curves in Fig. 4, the reliability and the reliability gain in MAC layer can be evaluated by Eq. (18). Fig. 5 shows that the reliability (*PRP* and *PRR*) from the theoretical model match with the simulation counterparts well. It is observed that the 5dB performance gain in 64QAM channel results in about 30.55% *PRP* gain and 14% *PRR* gain in MAC layer accounting for the impact of channel access and other network behaviors.

VI. CONCLUSIONS

The new SINR-based model that systematically analyzes the QoS metrics of IEEE 802.11 broadcast ad hoc networks is simpler and faster, more general, and more accurate compared with the existed SINR-based models. The analysis can be extended and used for the evaluation, design (planning), and real-time optimization of intelligent communication systems (IEEE 802.11p [6], IEEE 802.11bd [5]) in the future.

REFERENCES

[1] M. Ni, L. Cai, J. Yu, H. Wu, and Z. Zhang, Interference-based capacity analysis for vehicular ad hoc networks, *IEEE Commun. Lett.*, 19(4): 621-624, April 2015.
[2] X. Ma, H. Lu, J. Zhao, Y. Wang, J. Li, and M. Ni, Comments on "interference-based capacity analysis of vehicular ad hoc networks", *IEEE Commun. Lett.*, vol. 21, no. 10, pp. 2322-2325, Oct 2017.
[3] Z. Tong, H. Lu, M. Haenggi, and C. Poellabauer, A stochastic geometry approach to the modeling of DSRC for vehicular safety communication, *IEEE Trans. Intelligent Transportation Systems*, 17(5): 1448-1458, 2016.
[4] J. Zhao, Z. Wu, Y. Wang, and X. Ma, Adaptive Optimization of QoS Constraint Transmission Capacity of VANET, *Elsevier Vehicular Communications*, 17: 1-9, June 2019.
[5] B. Erdem, IEEE 802.11bd - A seamless evolutionary access layer for ITS-G5/DSRC, *CAR 2 CAR Journal*, 21-27, October 2019.
[6] X. Yin, X. Ma, and K. S. Trivedi, Interacting stochastic models approach for the performance evaluation of DSRC vehicular safety communication, *IEEE Trans. on Computers* 62(5): 873-885 (2013).
[7] Y. Yao, et al., Density-aware rate adaption scheme for vehicular safety communications in the highway environment, *IEEE Commun. Lett.*, 18(7): 1167 - 1170, July 2014.
[8] M. Haenggi, and R. K. Ganti, Interference in large wireless networks, *Foundations and Trends® in Networking*, 3(2): 127-248, 2019.
[9] IEEE 802.11, "IEEE standard - part 11: Wireless LAN medium access control (MAC) and physical layer (PHY) specications," *IEEE Std* 802.11-2016 (Revision of IEEE Std 802.11-2012), pp. 1-3534, Dec 2016.